Published in final edited form as:
Mol Microbiol. 2010 December ; 78(5): 1280–1293. doi:10.1111/j.1365-2958.2010.07407.x.

Nitric oxide sensitive and insensitive interaction of *Bacillus subtilis* NsrR with a ResDE-controlled promoter

Sushma Kommineni, **Erik Yukl**[Φ], **Takahiro Hayashi**, **Jacob Delepine**, **Hao Geng**[†], **Pierre Moënne-Loccoz**, and **Michiko M. Nakano**[*]
Department of Science & Engineering, School of Medicine, Oregon Health & Science University, 20000 NW Walker Road, Beaverton, OR 97006, USA

Summary

NsrR is a nitric oxide (NO)-sensitive transcription repressor that controls NO metabolism in a wide range of bacteria. In *Bacillus subtilis*, NsrR represses transcription of the nitrite reductase (*nasDEF*) genes that are under positive control of the ResD-ResE two-component signal transduction system. Derepression is achieved by reaction of NO with NsrR. Unlike some NsrR orthologues that were shown to contain a NO-sensitive [2Fe-2S] cluster, *B. subtilis* NsrR, when purified anaerobically either from aerobic or anaerobic *Escherichia coli* and *B. subtilis* cultures, contains a [4Fe-4S] cluster. [4Fe-4S]-NsrR binds to around the −35 element of the *nasD* promoter with much higher affinity than apo-NsrR and binding of [4Fe-4S]-NsrR, but not apo-protein, is sensitive to NO. RNA polymerase and phosphorylated ResD make a ternary complex at the *nasD* promoter and NsrR dissociates the preformed ternary complex. In addition to the −35 region, NsrR binds to two distinct sites of the upstream regulatory region where ResD also binds. These interactions, unlike the high-affinity site binding, do not depend on the NsrR [4Fe-4S] cluster and binding is not sensitive to NO, suggesting a role for apo-NsrR in transcriptional regulation.

Keywords

Bacillus subtilis; NsrR; ResD-ResE; nitric oxide; Fe-S cluster

Introduction

In order to adapt to oxygen limitation, *Bacillus subtilis* undergoes a global change in its transcriptional profile (Ye *et al.*, 2000). This includes the upregulation of genes specifying products that function in anaerobic respiration. The ResDE two-component signal transduction system composed of the ResE sensor kinase and the cognate ResD response regulator plays an important role in regulating anaerobic respiration as well as aerobic respiration (Nakano *et al.*, 1996, Sun *et al.*, 1996). ResE, upon sensing an unidentified signal, undergoes autophosphorylation and promotes phosphorylation of ResD. Phosphorylated ResD (ResD~P) activates transcription of genes involved in the respiratory pathway that transfers electrons to oxygen (under aerobic conditions) or to nitrate (under anaerobic conditions). Among ResDE-controlled genes, *nasDEF* and *hmp*, which encode nitrite reductase and flavohemoglobin respectively, are the most highly induced during nitrate respiration (Ye *et al.*, 2000) or by nitric oxide (NO) (Moore *et al.*, 2004, Nakano,

[*]For correspondence. mnakano@ebs.ogi.edu ; Tel. (+1) 503 748 4078; Fax (+1) 503 748 1464.
[†]Present address: Division of Hematology & Medical Oncology, Oregon Health & Science University, Portland, OR 97239, USA.
[Φ]Present address: Department of Biochemistry, Molecular Biology & Biophysics, University of Minnesota, Minneapolis, MN 55455, USA.

2002). Later studies showed that strong induction of these genes is caused by inactivation of the NO-sensitive NsrR transcriptional regulator (Nakano *et al.*, 2006, Yukl *et al.*, 2008).

NsrR belongs to a recently discovered family of transcription regulators that directly sense NO [reviewed in (Spiro, 2007)]. Investigators using a comparative genomic approach proposed that NsrR is a master regulator in NO metabolism both in gram-positive and gram-negative bacteria (Rodionov *et al.*, 2005). This was further confirmed by studies in various bacteria including *Escherichia coli* (Bodenmiller & Spiro, 2006, Filenko *et al.*, 2007, Rankin *et al.*, 2008), *Neisseria gonorrhoeae* (Isabella *et al.*, 2008, Isabella *et al.*, 2009, Overton *et al.*, 2006), *Neisseria meningitidis* (Heurlier *et al.*, 2008, Rock *et al.*, 2007), *Salmonella enterica* serovar *typhimurium* (Bang *et al.*, 2006), and *Moraxella catarrhalis* (Wang *et al.*, 2008) as well as in *B. subtilis* (Nakano *et al*., 2006). Survival of an *nsrR* mutant of *S. enterica* serovar Typhimurium in IFN-γ-stimulated macrophages was reduced compared to the wild-type strain due to enhanced sensitivity to oxidative stress (Gilberthorpe *et al.*, 2007), suggesting the importance of NsrR in bacterial pathogenesis. Transcription of NsrR-controlled genes is upregulated by either an *nsrR* null mutation or with NO, hence NsrR functions as a transcription repressor, the activity of which is sensitive to NO. The *B. subtilis nsrR* gene was originally identified by a transcription factor-transformation array analysis as the site of mutation that resulted in aerobic derepression of *hmp* (Nakano *et al*., 2006). NsrR represses ResD-controlled *nasDEF* and *hmp* transcription and repression is relieved by an exogenous NO donor (such as spermine NONOate) and endogenous NO that is produced by nitrate respiration.

Although the importance of NO in mammalian physiology and pathophysiology is well known [reviewed in (Gross & Wolin, 1995)], it has begun to emerge that NO also plays a pivotal role in bacterial physiology including bacterial infection and persistence in host organisms (Fang, 2004). As NO is an intermediate metabolite in denitrification and is freely diffusible across membranes, not only denitrifiers but also bacteria that cohabit with denitrifiers in various environments constantly encounter NO. Furthermore, it has been shown that even non-denitrifying bacteria endogenously produce NO during nitrate respiration (Ji & Hollocher, 1988). For example, *Salmonella* nitrate reductase (NarGHJI) (Gilberthorpe & Poole, 2008) and *E. coli* nitrite reductases (NrfA and NirB; Corker & Poole, 2003, Weiss, 2006) were shown to generate NO.

Our previous study showed that anaerobically purified *B. subtilis* NsrR (BsNsrR) bears a [4Fe-4S] cluster that, upon exposure to NO, forms dinitrosyl iron complexes (Yukl *et al*., 2008). Aerobically purified NsrR from *N. gonorrhoeae* (NgNsrR) (Isabella *et al*., 2009) and *Streptomyces coelicolor* (ScNsrR) (Tucker *et al.*, 2008) were shown to contain a NO-sensitive [2Fe-2S] cluster, causing some uncertainty as to the form of Fe-S cluster that is physiologically relevant. Here, we report that anaerobically purified BsNsrR (from either *E. coli* or *B. subtilis* cultures) contains a [4Fe-4S] cluster. We also demonstrate that NsrR binds around the −35 element of the *nasD* promoter and to a further upstream region that overlaps with the ResD-binding sites. The binding of NsrR to the −35 region is greatly enhanced by the presence of the [4Fe-4S] cluster, whereas the binding to the upstream region does not require the Fe-S cluster.

Results

Anaerobically purified NsrR either from aerobic or anaerobic E. coli cultures contains a [4Fe-4S] cluster

In order to eliminate the possibility that the [4Fe-4S] cluster detected with N-terminal and C-terminal His_6-tagged BsNsrR (Yukl *et al*., 2008) is the result of an erroneous Fe-S cluster formation, we constructed a C-terminal Strep-tag BsNsrR and purified the protein from *E.*

coli under anaerobic conditions. The Strep-tag BsNsrR, like the C-terminal His_6-tagged BsNsrR (Yukl *et al*., 2008), is functional when produced in *B. subtilis* (Fig. S2). Absorbance spectra in the visible region for Strep-tag NsrR showed that anaerobically purified protein has a [4Fe-4S] cluster like the His_6-tagged proteins (Fig. S1). The presence of a [4Fe-4S] cluster was further confirmed by resonance Raman (RR) spectroscopy (Fig. S1) and electron paramagnetic resonance (EPR) spectroscopy (data not shown). We also noted that even when *E. coli* cells were grown and handled aerobically prior to lysis, the [4Fe-4S]form of NsrR was observed if purified anaerobically, suggesting that native BsNsrR harbors a [4Fe-4S] cluster. These data ruled out any concern of interference from the His_6-tag on the Fe-S cluster, and subsequent experiments were carried out with the C-terminal His_6-NsrR (NsrR-His_6)protein.

The [4Fe-4S] cluster is required for high-affinity DNA-binding of NsrR

We examined whether the [4Fe-4S] cluster is essential for binding of NsrR to *nasD* by electrophoretic mobility shift assays (EMSA). As a probe, we used a 30-base pair double-stranded *nasD* DNA carrying the putative NsrR-binding site previously identified (Nakano *et al*., 2006) (−44 to −19 in Fig. 1). The double-stranded DNA was generated by annealing complementary oligonucleotides (Experimental procedures). Anaerobically purified [4Fe-4S]-NsrR (average [4Fe-4S]-cluster incorporation was 28%) bound to the double-stranded DNA (marked with *) and not to the single-stranded DNA (marked with **) (Fig. 2A). At 0.5 nM, [4Fe-4S]-NsrR began to bind *nasD* with apparent half-saturation that occurs between 2 and 8 nM depending on the NsrR preparation. Corrected for the amount of apo-protein present, the K_d of [4Fe-4S]-NsrR can be estimated to be below 2 nM. Two shifted bands with slightly different electrophoretic mobilities were observed and intensities of the faster migrating band increased as NsrR concentration increased. We assume that one of the shifted bands is likely the complex between target DNA and a heterodimer formed by [4Fe-4S]-NsrR and apo-NsrR for the following reasons. First, our previous result showed that NsrR forms a dimer regardless of the Fe-S cluster (Yukl *et al*., 2008). Second, both shifted bands are sensitive to spermine NONOate (see Fig. 4A), thus NsrR bound to the probe contains a Fe-S cluster, which is further supported by the finding that DNA-bound apo-NsrR migrates slower than the two shifted bands (data not shown). Excess amounts of cold *nasD* DNA competed for NsrR binding to the radioactive probe (Fig. 2E).

The aerobically purified NsrR (apo-NsrR) contains essentially no Fe-S cluster as judged by the measurement of Fe (less than 0.75% incorporation of the [4Fe-4S] cluster). The binding of apo-NsrR to *nasD* was much weaker compared to [4Fe-4S]-NsrR and the K_d was too high to be assigned at least within the range of concentrations used (Fig. 2B). These results demonstrated that the [4Fe-4S] cluster is essential for high-affinity binding of NsrR to the target promoter.

NsrR has three cysteines that likely serve to coordinate the [4Fe-4S] cluster. To assess the importance of cysteines for NsrR function, mutant NsrR proteins with Cys to Ala substitutions were produced. Western blot analysis showed that all mutant proteins were produced in *B. subtilis* (Fig. 3A). *nasD* expression was severely repressed in cells producing the wild-type NsrR, whereas the expression was derepressed in cells producing the mutant proteins to a level similar to that in the *nsrR* null mutant (Fig. 3B). This result demonstrated that the three cysteine residues are important for NsrR repressor activity.

The C100A mutant protein was purified from *E. coli* to determine whether the loss of repressor activity was caused by a weaker binding affinity for the *nasD* promoter due to the lack of the [4Fe-4S] cluster. No measurable iron was detected in the mutant protein when purified anaerobically by the same protocol as used for wild-type NsrR purification, suggesting that the cysteine is important for ligation of the [4Fe-4S] cluster. NsrR(C100A)

protein showed a weak DNA-binding activity equivalent to the aerobically purified apo-NsrR (compare Figs. 2B and 2C), confirming the requirement of the Fe-S cluster in efficient DNA binding to repress transcription.

Spermine NONOate abrogates binding of NsrR to nasD

To address the effect of NO on binding of NsrR to *nasD*, we used a NO donor spermine NONOate (hereafter referred to as SperNO). One mole of SperNO generates two moles of NO with a half-life of 39 min at 37°C and 230 min at 20–25°C (at pH 7.4, Cayman Chemical). Under our EMSA conditions, 1 μM or less NO is likely released from 10 μM SperNO solution. SperNO, at a concentration of 5 to 10 μM, inhibited the binding of [4Fe-4S]-NsrR (Fig. 4A) as seen by an increase of the free probe. At higher concentrations of SperNO, a small amount of a *nasD*-NsrR complex with a slower electrophoretic mobility appeared (marked with an arrow in Fig. 4A). This NO-induced complex migrated to the same position in a native gel as a complex formed with apo-NsrR (data not shown), suggesting that this complex was formed with *nasD* and apo-NsrR (see Fig. 7C as well). In contrast to [4Fe-4S]-NsrR, binding of apo-NsrR and NsrR(C100A) to *nasD* was not affected by SperNO (Figs. 4B and 4C). Taken together, these results clearly showed that the [4Fe-4S] cluster is essential for NO-responsive NsrR activity.

NsrR represses ResD-controlled nasD transcription in vitro and NO partially alleviates repression

To assess whether the EMSA results described above explain the negative effect of NsrR on *nasD* transcription as well as the antagonistic role of NO in NsrR-dependent repression, we performed *in vitro* transcription assays of *nasD*. Compared to apo-NsrR (Fig. 5B) and NsrR(C100A) (Fig. 5C), [4Fe-4S]-NsrR was able to repress the transcription at much lower concentrations (Fig. 5A). Quantitative analysis using ImageJ showed that minimal concentrations required for repression were slightly variable in the case of anaerobically purified NsrR, which is likely caused by variations in Fe-S cluster incorporation from prep to prep (Fig. 5A). SperNO at 20 μM largely relieved NsrR-dependent *nasD* repression (Fig. 5D), but had no significant effect on *nasD* transcription in the absence of NsrR, confirming that NO stimulates *nasD* transcription by alleviating NsrR-dependent repression. Transcription of *rpsD* encoding ribosomal protein S4 was not repressed by NsrR (Fig. 5E), which is consistent with *in vivo* result (Nakano *et al*., 2006).

NsrR inhibits the interaction of RNA polymerase-ResD~P with the nasD promoter and NO relieves the inhibition

The EMSA results described above argue that the binding of NsrR to the −35 region plays a pivotal role in NsrR-dependent repression of *nasD*. As the ResD-ResE signal transduction proteins are essential for activation of *nasD* (Nakano *et al.*, 1998), we examined how NsrR interferes with ResD-dependent transcription of *nasD*. To this end, anaerobic EMSA experiments were carried out with a longer *nasD* (−114 to −4) probe that also includes the previously identified ResD-binding region (Geng *et al.*, 2004, Nakano *et al.*, 2000) (Fig. 1). ResD~P alone at 0.5 μM did not bind to the *nasD* promoter, whereas RNA polymerase (RNAP) as low as 15 nM interacted with the probe (shown by the arrow with #1 in Fig. 6A). When RNAP was present, 0.5 μM ResD~P supershifted the *nasD*-RNAP complex (the arrow with #2). These data suggested that the role of ResD~P in *nasD* transcription is not simply to recruit RNAP to the promoter.

To determine whether [4Fe-4S]-NsrR disrupts the preformed *nasD*-RNAP-ResD~P transcription initiation complex, we allowed the *nasD*-RNAP-ResD~P ternary complex to form, followed by addition of NsrR. NsrR at 2 nM started to bind the probe and increasing concentrations of NsrR displaced the preformed ternary complex, which was accompanied

by formation of multiple *nasD*-NsrR complexes (the arrow with #3 in Fig. 6B). These results indicated that [4Fe-4S]-NsrR efficiently disrupts the *nasD*-RNAP-ResD~P initiation complex by binding to the *nasD* promoter and that the second and third NsrR-binding sites exist in the region between −114 and −4 (Fig. 6B). The *nasD*-RNAP complex was also disrupted in the presence of 8 nM NsrR, and a small amount of a supershifted band appeared at higher concentrations of NsrR (the arrow with #2 in Fig. S3A). This band could represent *nasD*-RNAP-NsrR complex resulted from binding of apo-NsrR to the upstream *nasD* as described later. Although ResD~P does not efficiently bind to *nasD* as shown in Figure 6A, it weakly binds at 1 μM (the arrow with #4 in Fig. S3B). In the presence of 2 nM NsrR, a supershifted band appeared, which was likely formed by binding of ResD~P and [4Fe-4S]-NsrR to *nasD*.

As observed in EMSA using a shorter probe (Fig. 4A), the presence of SperNO at concentrations of 20 to 40 μM and higher altered the electrophoretic mobility of the *nasD*-NsrR complexes (shown with solid arrows in Fig. 7), generating new complexes (broken arrows) with slower mobilities. At these SperNO concentrations, we also observed a simultaneous increase in the amount of *nasD*-RNAP-ResD~P ternary complex and free probe (Fig. 7A). Similarly, SperNO restored *nasD*-RNAP binary complex formation (Fig. 7B). SperNO showed no significant effect on the binding of either RNAP alone or RNAP-ResD~P to *nasD* (data not shown), demonstrating that SperNO is directed only at [4Fe-4S]-NsrR.

What is the nature of the *nasD*-NsrR complex generated by SperNO? Figure 7C shows that the complexes formed by anaerobically purified NsrR in the presence of SperNO migrated at the same position in a native gel as those formed by aerobically purified apo-NsrR. In this experiment we used 128 nM NsrR, the concentration of which was shown to be sufficient for apo-NsrR to bind to *nasD* (Fig. 2B). As shown in Figure 2B, 8 nM apo-NsrR is unable to bind the *nasD* probe carrying only the primary NsrR-binding site. If the shifted band with the slowest mobility that was generated by SperNO is indeed the *nasD*-apo-NsrR complex, then the band should not be generated when 8 nM NsrR is used. The result showed that it is indeed the case (data not shown). Therefore, the SperNO-induced *nasD*-NsrR complexes in Figures 4A and 7 are likely formed with apo-NsrR either present in anaerobically purified NsrR protein or generated by SpeNO, although we could not completely eliminate the possibility that the complex contains DNIC-NsrR.

Apo-NsrR binds to the ResD-binding region of nasD

The results described in Figures 6 and 7 suggested that NsrR interacts with *nasD* by binding to the second and third sites in addition to the primary site around the −35 region. To understand the role of the secondary binding sites in regulation of *nasD* transcription, we determined the location of the secondary NsrR-binding sites and whether binding affinities of these *cis* elements are different between [4Fe-4S]-NsrR and apo-NsrR. To localize the secondary sites, we generated a probe (−114 to −40) that lacks the primary NsrR-binding site. Three important results were obtained by comparing EMSA results of NsrR between the full-length (−114 to −4) probe and the deleted (−114 to −40) probe. First, at higher concentrations of NsrR, three *nasD*-NsrR complexes were formed with the full-length probe, while only two complexes were detected with the deleted probe (Fig. 8). Based on this result, we concluded that the second and third NsrR-binding sites locate in the region between −114 and −40. Second, when the full-length probe was used, the *nasD*-NsrR complex with the fastest mobility (marked as #1 in Fig. 8A) was formed with [4Fe-4S]-NsrR at much lower concentrations than with apo-NsrR (compare Figs. 8A and 8B), whereas [4Fe-4S]-NsrR and apo-NsrR bound to the deleted probe with a similar affinity to form the first complex (marked #2/3, and compare Figs. 8D and 8E). Furthermore, apo-NsrR bound similarly to these three sites (compare Fig. 8B and 8E). These results argued that the NsrR-

binding site around the −35 element is the only site that [4Fe-4S]-NsrR binds with a higher affinity than apo-NsrR does. Third, the *nasD* promoter lacking the primary NsrR-binding site did not generate NO-specific complexes with slow elecrophoretic mobilities (compare Figs. 8C and 8F), which is in good agreement with the interaction of apo-NsrR with the upstream binding sites.

To further define the location of the upstream NsrR-binding sites, we generated four overlapping short double-stranded oligonucleotides that cover the region between −114 to −40 of *nasD* (Fig. 1). To determine with which probe apo-NsrR interacts, we performed EMSA experiment (Fig. S4). The result showed that the two binding sites reside in −93 to −63 and −71 to −40 of *nasD*. The probe from −104 to −75 exhibited a very weak activity, suggesting that the region between −93 and −75 serves as a core-binding site and DNA from −74 to −63 is required for stabilizing the *nasD*-NsrR complex. EMSA using [4Fe-4S]-NsrR showed an almost identical result (data not shown). Interestingly the region from −93 to −40 where apo-NsrR binds was identified as the ResD-binding site in our previous studies (Geng *et al*., 2004,Nakano *et al*., 2000).

A high concentration of NsrR is detected in B. subtilis cells

The results described above showed that apo-NsrR binds to the *nasD* regulatory region that overlaps with ResD-binding site. The question remains whether the interaction between apo-NsrR and *nasD* is physiologically relevant, particularly because the affinity of apo-NsrR to these sites is weaker than that of [4Fe-4S]-NsrR to the primary binding element. To evaluate whether there is a good possibility that the apo-NsrR-DNA interaction occurs *in vivo*, we measured NsrR concentration in *B. subtilis* cells using quantitative western blotting as previously described (Cai & Inouye, 2002) with some modification (Experimental procedures) (Fig. 9). As a standard, we used various concentrations of the purified NsrR-His_6 protein. The cell lysate prepared from *B. subtilis* JH642 was resolved on an SDS-PAGE gel together with the standard NsrR protein. Polyclonal anti-His_6-NsrR antiserum (Nakano *et al*., 2006) was used to determine concentrations of NsrR in the western blot. We repeated the experiments using three independently prepared cell lysate and three different purification batches of NsrR proteins as standards. The aqueous volume of a *B. subtilis* cell was estimated as 1×10^{-14} liter by previous study (McCabe & Gollnick, 2004). By calculating with this value of cell volume, we found that in vivo NsrR concentration is 1.34 ± 0.21 μM (n=7), which corresponds to 8,066 ± 1,264 monomers in the cell. The result, together with the EMSA result in Figure 8, suggests that the cellular NsrR concentration is likely sufficient to allow NsrR to interact with low-affinity binding sites of *nasD*.

Discussion

The NO-sensitive transcription regulator NsrR plays an important role in the control of the NO stress response in a wide range of bacteria [reviewed in (Tucker *et al.*, 2010)]. We presented data here to confirm our earlier study (Yukl *et al*., 2008) that *B. subtilis* NsrR proteins, when purified from either aerobic or anaerobic *E. coli* cultures, carry a [4Fe-4S] cluster. In addition, while revising this manuscript, we successfully purified the C-terminal His_6-NsrR from *B. subtilis* (see supporting information). NsrR purified from the native host carries a [4Fe-4S] cluster and the Fe-S incorporation (average 65%) was much higher than the heterologously expressed protein (average 28%). The NsrR protein behaves similarly to the protein purified from *E. coli* with respect to DNA-binding activity and NO sensitivity (Fig. S5). From these results we conclude that Bs-NsrR contains a [4Fe-4S] cluster in *B. subtilis*. The [4Fe-4S] cluster is maintained in aerobic cultures presumably because the concentration of intracellular oxygen remains sufficiently low. In addition, glutathione was postulated to be involved in stabilizing or reactivating oxidized Fe-S clusters (Song *et al.*, 2006) and a similar role might be played by low-molecular-weight thiols such as cysteine

and bacillithiol (Newton *et al*., 2009) in *B. subtilis* that lacks glutathione. In either case, the higher *in vivo* sensitivity of NsrR to NO than to oxygen is apparent from the previous *in vivo* result that ResD-independent *hmp* expression is repressed by NsrR in *B. subtilis* cells cultured aerobically and the repression is relieved by SperNO (Nakano *et al*., 2006).

Although NsrR-dependent repression of *nasD* is relieved by SperNO, NO-dependent upregulation of *nasD* transcription still requires ResD. We have previously shown that certain amino acid residues of the carboxy-terminal domain of the α subunit (αCTD) are required for ResD-dependent transcription of *fnr* (Geng *et al.*, 2007) and *nasD* (H.G. and M.M.N. unpublished results). Transcriptional activators that requireαCTD are known to bind upstream of the −35 element and recruit RNAP via interaction with αCTD (Busby & Ebright, 1999). This recruitment model of gene activation could not explain how ResD~P plays a role in activation of *nasD*, as RNAP alone binds to *nasD* and stimulates binding of ResD~P to *nasD* (Fig. 6A). We noticed that the *nasD* promoter contains a 5′-TtTG-3′ sequence one base pair upstream of the −10 hexamer (5′-TGTGCT-3′) (the downstream 5′-TGCTACGCT-3′ sequence, which overlaps with the putative −10 sequence, could also serve as an extended −10 promoter). “Extended −10 promoters” carrying the 5′-TG-3′ (and often 5′-TRTG-3′) motif have been found in *E. coli* (Mitchell *et al.*, 2003) and are more common in *B. subtilis* (Helmann, 1995, Voskuil & Chambliss, 1998). *E. coli* extended −10 promoters generally show weak matches to the consensus −35 element, whereas *B. subtilis* extended −10 promoters have highly conserved −35 sequences. Given that the *nasD* promoter contains a non-canonical −10 hexamer (TGTGCT) and lacks −35 hexamer, one could envisage that the interaction between ResD~P and αCTD assists in productive binding of RNAP to *nasD*.

This study showed that the preformed *nasD*-RNAP-ResD~P complex is dissociated by NsrR (Fig. 6B), partly, if not solely, by competing with RNAP for interaction with the high-affinity NsrR-binding site (−39 and −24) (Fig. S3). The ternary complex formation was more strongly inhibited by the higher concentrations of NsrR that promotes secondary site binding (Fig. 6B). The secondary sites were localized in two distinct regions, within −93 to −63 and −71 to −40, which overlap the previously identified ResD-binding region (around −91 to −46). Neither apo-NsrR nor [4Fe-4S]-NsrR bound the *nasD*(−114 to −85) fragment, indicating that apo-NsrR interacts with the secondary sites in a sequence-specific manner. Interestingly, anaerobically purified NsrR and aerobically purified NsrR bind with a similar affinity to these secondary sites, which is in sharp contrast to the primary NsrR-binding site where the [4Fe-4S] cluster is required for efficient binding.

There is a precedent for both holo- and apo-forms of Fe-S transcription regulator playing roles in gene regulation. *E. coli* IscR, a [2Fe-2S] cluster-carrying transcription regulator (Schwartz *et al.*, 2001), and NsrR are similar in primary structure. IscR controls transcription of the *iscRSUA* and *sufABCDSE* operons encoding proteins that function in assembly of Fe-S clusters. Under oxidative stress and iron limiting conditions, apo-IscR activates *sufA* transcription (Yeo *et al.*, 2006) and [2Fe-2S]-IscR-dependent repression of *iscR* is concomitantly relieved (Giel *et al.*, 2006) in order to meet the cell’s need for Fe-S reassembly. The two forms of IscR recognize sequences specific to promoters of each class (Giel *et al*., 2006, Nesbit *et al.*, 2009). A partial inverted repeat sequence ATRTATYTtAAATATAT was previously proposed as a putative *B. subtilis* NsrR-binding site (Nakano *et al*., 2006). Consistent with this notion, [4Fe-4S]-NsrR preferentially binds a 30-mer oligonucleotide that includes the putative binding site (Fig. 1 and Fig. 2). The EMSA results in Figure S4 (and see Fig. 1 for sequence) indicated that apo-NsrR-binding elements reside within two separate 30 nucleotide regions. We could not find high sequence similarity between the sites recognized by apo-NsrR and the [4Fe-4S]-NsrR-binding element. The two

regions recognized by apo-NsrR show some similarity (Fig. 1), but further study is required to deduce the consensus binding sequence for apo-NsrR.

The observation that anaerobically and aerobically purified NsrR bound to the upstream sites with a similar affinity raises two alternative possibilities. One possibility is that apo- and [4Fe-4S]-NsrR indeed have a similar affinity to these sites. The other possibility is that apo-NsrR binds with a higher affinity than [4Fe-4S]-NsrR. A larger population of apo-NsrR present in anaerobically purified NsrR made it difficult to measure the binding affinity of [4Fe-4S]-NsrR in anaerobically purified protein sample. Although we could not eliminate the former possibility, we assume the latter possibility is more likely. The EMSA result with the probe (−114 to −40) lacking the high-affinity binding site indicated that the *nasD* complex formed by anaerobically purified NsrR did not promote the supershift usually observed in the presence SperNO (Fig. 8F and compare with Fig. 8C). The result suggests that NsrR molecules bound to the probe were almost exclusively apo-protein, in keeping with the preferential recognition of the two upstream binding sites by apo-NsrR. In the case of IscR, a recent study showed that both apo- and [2Fe-2S]-IscR bind to *sufA*-class promoters in a sequence-specific manner (Nesbit *et al*., 2009).

To our knowledge, this is the first report suggesting that apo- and [Fe-S]-NsrR interact with two distinct classes of DNA targets that have different recognition sequences. Furthermore, instead of separate sets of genes, the two classes of NsrR-target sequences reside in the single *nasD* gene promoter region. It remains to be determined what function these two NsrR-target sites perform in the regulation of *nasD* expression. Assuming that apo-NsrR concentration increases relative to [4Fe-4S]-NsrR under conditions that disrupt the Fe-S cluster formation, one could envisage apo-NsrR occupying the ResD-binding region. Simultaneously, RNAP might successfully compete for the −35 region to which apo-NsrR weakly binds. The outcome is that, instead of a *nasD*-RNAP-ResD complex, a *nasD*-RNAP-NsrR complex might be formed to initiate *nasD* transcription. This is a very speculative view but is worth examining in future. The results of this study also suggest that apo-NsrR might function independently of holo-NsrR in regulation of yet-unidentified genes.

Experimental procedures

Bacterial strains and culture conditions

The strains and plasmids used in this study are listed in Table S1. *E. coli* DH5α was used for cloning of the recombinant plasmids. *E. coli* BL21 (DE3)/pLysS was used to produce NsrR proteins and ER2566 (New England Biolabs) was used for production of ResD and ResE. All *B. subtilis* strains are isogenic derivatives of JH642. ORB6559 was constructed by transforming pCm::Sp (Steinmetz & Richter, 1994) into ORB6179 (Nakano *et al*., 2006), which replaces the chloramphenicol-resistance marker in *nsrR* with spectinomycin resistance. Antibiotic concentrations used in growth media were ampicillin (50 μg ml^{-1}), chloramphenicol (5 μg ml^{-1}), spectinomycin (75 μg ml^{-1}), and erythromycin/lincomycin (1 μg $ml^{-1}$and 25 μg ml^{-1}, respectively).

Alanine substitutions of cysteine residues in NsrR

In order to substitute each cysteine in NsrR (amino acid residues 92, 100, and 106) and ectopically express the mutant *nsrR* genes in strain ORB6559 (*nsrR:spc*), the following plasmids were constructed using a *thrC* integration vector pDG795 (Guérout-Fleury *et al.*, 1996). Plasmids pHG64 and pHG66, pUC18 derivatives carrying *nsrR*(C92A) and *nsrR*(C106A) respectively, were digested with EcoRI and BamHI and the *nsrR* genes were inserted into pDG795 digested with the same enzymes to generate pMMN666 and pMMN667, respectively. pDG795 carrying *nsrR*(C100A) was generated by two-step PCR as

follows. Two PCR products amplified from pHG56 using oligonucleotide pairs − oHG89 (5′-AAGAATCTCGCTGTTATTTCCCCGGTT-3′)/oHG94 (5′-GA*GGATCC*GCTTTTGAC CTT-3′: BamHI site is italicized) and oHG90 (5′-AACCGGGGAAATAACAGCGAGA TTCTT-3′)/oHG93 (5′-CG*GAATTC*GCACTTGCTTTC-3′: EcoRI site is italicized). The PCR products were annealed and used as template in the second PCR with oHG93 and oHG94 as primers. The resultant PCR product was digested with EcoRI and BamHI and inserted into EcoRI/BamHI-cleaved pDG795, resulting in pMMN669. A pDG795 derivative carrying *nsrR*(wt), pMMN668, was constructed by subcloning the *nsrR* gene from pHG56 into pDG795 in a similar way described above. *nsrR* in each plasmid was verified by sequencing analysis. These four pDG795 derivatives were used to transform ORB6559 (*nsrR::spc*) with selection for erythromycin- and spectinomycin-resistance and Thr¯colonies generated by a double-crossover recombination were chosen as ORB6629 [*nsrR::spc thrC::nsrR*(C92A)], ORB6630 [*nsrR::spc thrC::nsrR*(C106A)], ORB6631 [*nsrR::spc thrC::nsrR* (wt)], and ORB6632 [*nsrR::spc thrC::nsrR*(C100A)]. Strains ORB6629 to 6632 were transduced by SPβ phage carrying *nasD-lacZ* (Nakano *et al*., 1998) to generate ORB6640 to 6643, respectively.

β-Galactosidase activity measurement

Two independent isolates of each *B. subtilis* strain were cultured at 37°C under anaerobic conditions in 2x yeast extract-tryptone (YT) media (Nakano *et al.*, 1988) with 0.5% glucose and 0.5% pyruvate supplemented with antibiotics, if necessary. Cells were harvested at 1-h intervals and β-galactosidase activity was measured as described (Miller, 1972). The activity at T1 (1 h after the end of the exponential growth) was shown.

Western blot analysis

Cells were cultured at 37°C in 2xYT supplemented with 0.5% glucose, 0.5% pyruvate, and appropriate antibiotics. When the optical density at 600 nm (OD_{600}) of the cultures reached approximately 0.4, cells were harvested and cell lysate was prepared by passing through a French press. Twentyμg of total protein was applied to sodium dodecylsulfate-polyacrylamide (15%) (SDS-PAGE) gel and western blot analysis was carried out using anti-His_6-NsrR antibody as described (Nakano *et al*., 2006).

Determination of cellular concentration of NsrR by quantitative western blot analysis

The intracellular concentration of NsrR was determined in JH642 cells grown anaerobically in 2xYT supplemented with 0.5% glucose and 0.5% pyruvate. Cells were harvested at OD_{600}=0.4 to 0.5, and cell lysate was prepared from the 45-ml cultures using the protoplast lysis method as previously described (Baruah *et al.*, 2004). Around 15 μg of total protein in 15 μl was applied to a 15% SDS-PAGE. NsrR-His_6 was purified as described below and 0.0625 to 2 pmoles protein in 15 μl was used as standard. Detection of NsrR was carried out by western blot using anti-His_6-NsrR antibody as described (Nakano *et al*., 2006). Colony-forming units were determined from the cultures by serial dilution and plating on LB agar.

Anaerobic and aerobic purification of NsrR-His_6

NsrR-His_6 protein was overproduced in *E. coli* BL21(DE3)/pLysS carrying pMMN740 as previously described (Yukl *et al*., 2008). For anaerobic protein purification, cell pellet was transferred to an anaerobic chamber (Coy Laboratory Products) containing 5% H_2 and 95% N_2, where the centrifuge tube was kept with its lid open until chamber oxygen level was below 5 ppm. Cell suspension was transferred into a French press cell and all French press cell components were assembled in the anaerobic chamber. Cell lysate obtained by passage through the French press was collected into a centrifuge tube while being purged with N_2.

Aerobic purification was performed outside the anaerobic chamber in the same way as anaerobic purification.

The NsrR(C100A) mutant protein was purified from BL21(DE3)/pLysS carrying pMMN805 under anaerobic conditions following the same procedure as for wild-type NsrR. To construct pMMN805, *nsrR*(C100A) was amplified by PCR using oMN05-296 (5′-GGCGCGGG*CATATG*AAGTTAACCAATTATAC-3′: NdeI site is italicized) and oMN05-304 (5′-CGCT*CTCGAG*TTCCTTCATTTTTAAAAGC-3′: XhoI site is italicized) with pMMN732 as template. The PCR product digested with NdeI and XhoI was inserted into pET23a(+) digested with the same enzymes to generate pMMN805. The *nsrR* coding sequence was confirmed by sequencing.

Purification of ResD, ResE, RNAP, and σ^A

ResD and ResE were overproduced in *E. coli* ER2566 (New England Biolabs) and purified as previously described (Geng *et al*., 2004) except that ResD protein was dialyzed against 25 mM Tris-HCl buffer (pH 8.0) containing 50 mM NaCl, 5 mM $MgCl_2$, 5% glycerol, and 5 mM β-mercaptoethanol before storage at −80°C. RNAP and σ^A were purified as previously described (Nakano *et al*., 2006).

Measurement of protein concentration and iron content

Protein concentrations were determined by Bio-Rad protein assay using bovine serum albumin as a standard. As seen with N-terminal His_6-NsrR (Yukl *et al*., 2008), total amino acid analysis of the C-terminal His_6-NsrR (AAA Service Laboratory Inc., Damascus, Oregon) showed that the Bio-Rad protein assay overestimates NsrR concentrations by ~26%. [4Fe-4S]-NsrR concentrations were calculated accordingly. The iron content of NsrR at two different protein concentrations (1 and 4 μM for anaerobically purified protein and 10 and 20 μM for C100A mutant and aerobically purified protein) was determined with a ferene assay as described (Yukl *et al*., 2008) and QuantiChrom iron assay kit (BioAssay Systems). The minimum amount detected was around 0.45 μM. Both methods gave similar results.

Electrophoretic mobility shift assay (EMSA) of NsrR, ResD~P and RNAP

EMSA was carried out under anaerobic and aerobic conditions as previously described except that the reaction buffer was slightly modified [50 mM Tris-HCl, pH 7.5, 100 mM KCl, 0.5 mM DTT, 5 mM $MgCl_2$, 5 μg ml^{-1} BSA, 10 μg ml^{-1} poly(dI-dC), 10% glycerol] and native gels were run in TGE buffer (50 mM Tris, 0.38 M glycine, 2 mM EDTA; pH not adjusted). For anaerobic experiments, EMSA was performed in the anaerobic chamber as carried out with other Fe-S proteins (Edwards *et al.*, 2010, Reents *et al.*, 2006). The solutions and electrophoresis buffer were degassed by purging with N_2 and were transferred to the anaerobic chamber one day before the experiment. Polyacrylamide gels assembled with the electrophoresis apparatus were placed in the anaerobic chamber and allowed to stand for at least 2 to 3 h before the gel was pre-run at 150 V for 1h. For EMSA using only NsrR, a shorter *nasD* probe (−45 to −20) was generated by annealing complementary 30-mer oligonucleotides oMN09-489 (5′-GCATAACATGTATCTTAAATATTCCTTTCG-3′; coding strand) and oMN09-491 (5′-CGAAAGGAATATTTAAGATACATGTTATGC-3′; noncoding strand). The annealed oligonucleotides cover the putative NsrR-binding site of *nasD* (Nakano *et al*., 2006). oMN09-489 (2 μM) was radiolabelled using 50 μCi [γ-^{32}P]-ATP (800 Ci/mmol) and T4 polynucleotide kinase at 37°C for 30 min. The reaction was stopped by heating at 65°C for 15min. The labelled oligonucleotide was purified using nucleotide removal kit (Qiagen) and was mixed with 2 μM of unlabelled oMN09-491 in New England Biolabs restriction enzyme buffer 2. To anneal the oligonucleotides, the mixture was heated at 90°C for 5 min in a heat block filled with water and the heat block was removed from the apparatus to slowly cool to the room temperature. Four probes (−114

to −85, −104 to −75, −93 to −63, and −71 to −40) used in the experiment of Figure S4 were generated similarly by annealing a labelled oligonucleotide shown in Figure 1 and the complementary unlabelled noncoding strand. Approximately 0.1 nM of the probe was used in 20 μl of the reaction buffer without or with NsrR.

For EMSA using ResD~P, RNAP, and NsrR, a longer *nasD* probe (−114 to −4) containing ResD-binding sites (Geng *et al*., 2004, Nakano *et al*., 2000) and the NsrR-binding site was generated as follows. Oligonucleotide oSK42 (5′-CCGTCCGAATCATACCTATT-3′) was radiolabelled using T4 polynucleotide kinase and [γ-^{32}P]-ATP. The probe DNA was generated by PCR from pMMN406 (Nakano *et al*., 2000) using labelled oSK42 and unlabelled oSK43 (5′-AGCGTAGCACAGCAAAAAGG-3′). The amplified PCR product was purified by PCR purification kit (Qiagen). A *nasD* probe (−114 to −40) that lacks the primary NsrR-binding site was similarly generated using oligonucleotides oSK42 and oSK79 (5′-GTTATAAAATGTAACAAAATATACG-3′).

To determine the effect of NsrR on a preformed *nasD*-RNAP complex, the *nasD* probe (around 0.2 nM) and RNAP (15 nM) were mixed in 20 μl of the EMSA reaction buffer. To determine the effect on the *nasD*-ResD~P, or *nasD*-RNAP-ResD~P complex, ResD (0.5 μM) was phosphorylated with ResE (0.5 μM) in 20 μl of the EMSA reaction buffer, to which *nasD* probe and RNAP (for the ternary complex formation) were added. The reaction mixture containing the preformed binary or ternary complex was incubated for 10 min at room temperature. Increasing concentrations of NsrR were added to the reaction, which was further incubated for 15 min. To examine the effect of NO, SperNO (dissolved in 10 mM NaOH) was added to the reaction 10 min after the addition of NsrR, and incubated at room temperature for additional 20 min. As a control 10 mM NaOH at the same volume as the SperNO solution was included in the reaction. After complexes were resolved by polyacrylamide gel electrophoresis, the gel was dried and radioactive bands were analysed with a Typhoon Trio^{+} variable imager (GE Healthcare). The intensity of bands was quantified using ImageJ (NIH).

In vitro transcription assay

The effect of NsrR on ResD-activated *nasD* transcription was determined using *in vitro* transcription assays as previously described (Nakano *et al*., 2006) with minor modifications. In short, a *nasD* template (−170 to +96 with respect to the transcription start site) was generated by PCR using oSK-34 (5′-TTTAATCGGGGAAGCCTTAGA-3′) and oHG-1 (5′-TATCTCTTCAATGGCCCTTA-3′) and purified by low-melting agarose gel and PCR purification kit (Qiagen). As a control, an *rpsD* promoter template was generated by PCR using oSN03-86 and oSN03-87 (Nakano *et al*., 2006). All reactions were performed in the Coy anaerobic chamber except otherwise stated. ResD (1 μM) and ResE (1 μM) were mixed in the transcription buffer (Nakano *et al*., 2006) containing RNasin (Promega) and incubated at room temperature for 10 min. Then 5 nM of the *nasD* template, NsrR at different concentrations, RNAP (15 nM), and σ^{A} (7.5 nM) were added and incubated at room temperature for 10 min, followed by the addition of SperNO, where indicated. Transcription was initiated by adding [α-^{32}P]-UTP and NTPs. The reaction mixture was further incubated for 10 min. After the reaction was stopped, samples were taken out from the chamber, precipitated with ethanol, and separated on a pre-run 6% polyacrylamide-urea gel at 500 V for approximately 40 min. The gel was dried and analysed with a Typhoon Trio^{+} variable imager and the intensity of bands was quantified using ImageJ.

Supplementary Material

Refer to Web version on PubMed Central for supplementary material.

Acknowledgments

We thank Peter Zuber for valuable comments on the manuscript and Cole Zuber for technical assistance. This work was supported in part by a grant GM74785 (P.M-L.) from the National Institute of Health, MCB0110513 (M.M.N.) from the National Science Foundation, and Vertex pharmaceutical scholarship (T.H.).

References

Bang IS, Liu L, Vazquez-Torres A, Crouch ML, Stamler JS, Fang FC. Maintenance of nitric oxide and redox homeostasis by the *Salmonella* flavohemoglobin *hmp*. J Biol Chem. 2006; 281:28039–28047. [PubMed: 16873371]

Baruah A, Lindsey B, Zhu Y, Nakano MM. Mutational analysis of the signal-sensing domain of ResE histidine kinase from *Bacillus subtilis*. J Bacteriol. 2004; 186:1694–1704. [PubMed: 14996800]

Bodenmiller DM, Spiro S. The *yjeB* (*nsrR*) gene of *Escherichia coli* encodes a nitric oxide-sensitive transcriptional regulator. J Bacteriol. 2006; 188:874–881. [PubMed: 16428390]

Busby S, Ebright RH. Transcription activation by catabolite activator protein (CAP). J Mol Biol. 1999; 293:199–213. [PubMed: 10550204]

Cai SJ, Inouye M. EnvZ-OmpR interaction and osmoregulation in *Escherichia coli*. J Biol Chem. 2002; 277:24155–24161. [PubMed: 11973328]

Corker H, Poole RK. Nitric oxide formation by *Escherichia coli*. Dependence on nitrite reductase, the NO-sensing regulator Fnr, and flavohemoglobin Hmp. J Biol Chem. 2003; 278:31584–31592. [PubMed: 12783887]

Edwards J, Cole LJ, Green JB, Thomson MJ, Wood AJ, Whittingham JL, Moir JW. Binding to DNA protects Neisseria meningitidis fumarate and nitrate reductase regulator (FNR) from oxygen. J Biol Chem. 2010; 285:1105–1112. [PubMed: 19917602]

Fang FC. Antimicrobial reactive oxygen and nitrogen species: concepts and controversies. Nat Rev Microbiol. 2004; 2:820–832. [PubMed: 15378046]

Filenko N, Spiro S, Browning DF, Squire D, Overton TW, Cole J, Constantinidou C. The NsrR regulon of *Escherichia coli* K-12 includes genes encoding the hybrid cluster protein and the periplasmic, respiratory nitrite reductase. J Bacteriol. 2007; 189:4410–4417. [PubMed: 17449618]

Geng H, Nakano S, Nakano MM. Transcriptional activation by *Bacillus subtilis* ResD: Tandem binding to target elements and phosphorylation-dependent and -independent transcriptional activation. J Bacteriol. 2004; 186:2028–2037. [PubMed: 15028686]

Geng H, Zhu Y, Mullen K, Zuber CS, Nakano MM. Characterization of ResDE-dependent fnr transcription in *Bacillus subtilis*. J Bacteriol. 2007; 189:1745–1755. [PubMed: 17189364]

Giel JL, Rodionov D, Liu M, Blattner FR, Kiley PJ. IscR-dependent gene expression links iron-sulphur cluster assembly to the control of O_2-regulated genes in *Escherichia coli*. Mol Microbiol. 2006; 60:1058–1075. [PubMed: 16677314]

Gilberthorpe NJ, Lee ME, Stevanin TM, Read RC, Poole RK. NsrR: a key regulator circumventing *Salmonella enterica* serovar Typhimurium oxidative and nitrosative stress in vitro and in IFN-gamma-stimulated J774.2 macrophages. Microbiology. 2007; 153:1756–1771. [PubMed: 17526833]

Gilberthorpe NJ, Poole RK. Nitric oxide homeostasis in *Salmonella typhimurium*: roles of respiratory nitrate reductase and flavohemoglobin. J Biol Chem. 2008; 283:11146–11154. [PubMed: 18285340]

Gross SS, Wolin MS. Nitric oxide: pathophysiological mechanisms. Annu Rev Physiol. 1995; 57:737–769. [PubMed: 7539995]

Guérout-Fleury AM, Frandsen N, Stragier P. Plasmids for ectopic integration in *Bacillus subtilis*. Gene. 1996; 180:57–61. [PubMed: 8973347]

Helmann JD. Compilation and analysis of *Bacillus subtilis* sigma A-dependent promoter sequences: evidence for extended contact between RNA polymerase and upstream promoter DNA. Nucleic Acids Res. 1995; 23:2351–2360. [PubMed: 7630711]

Heurlier K, Thomson MJ, Aziz N, Moir JW. The nitric oxide (NO)-sensing repressor NsrR of *Neisseria meningitidis* has a compact regulon of genes involved in NO synthesis and detoxification. J Bacteriol. 2008; 190:2488–2495. [PubMed: 18245279]

Isabella V, Wright LF, Barth K, Spence JM, Grogan S, Genco CA, Clark VL. cis- and trans-acting elements involved in regulation of *norB* (*norZ*), the gene encoding nitric oxide reductase in *Neisseria gonorrhoeae*. Microbiology. 2008; 154:226–239. [PubMed: 18174141]

Isabella VM, Lapek JD Jr, Kennedy EM, Clark VL. Functional analysis of NsrR, a nitric oxide-sensing Rrf2 repressor in *Neisseria gonorrhoeae*. Mol Microbiol. 2009; 71:227–239. [PubMed: 19007408]

Ji XB, Hollocher TC. Reduction of nitrite to nitric oxide by enteric bacteria. Biochem Biophys Res Commun. 1988; 157:106–108. [PubMed: 3058123]

McCabe BC, Gollnick P. Cellular levels of *trp* RNA-binding attenuation protein in *Bacillus subtilis*. J Bacteriol. 2004; 186:5157–5159. [PubMed: 15262953]

Miller, JH. Experiments in molecular genetics. Cold Spring Harbor Laboratory; Cold Spring Harbor, N.Y: 1972.

Mitchell JE, Zheng D, Busby SJ, Minchin SD. Identification and analysis of 'extended -10' promoters in *Escherichia coli*. Nucleic Acids Res. 2003; 31:4689–4695. [PubMed: 12907708]

Moore CM, Nakano MM, Wang T, Ye RW, Helmann JD. Response of *Bacillus subtilis* to nitric oxide and the nitrosating agent sodium nitroprusside. J Bacteriol. 2004; 186:4655–4604. [PubMed: 15231799]

Nakano MM. Induction of ResDE-dependent gene expression in *Bacillus subtilis* in response to nitric oxide and nitrosative stress. J Bacteriol. 2002; 184:1783–1787. [PubMed: 11872732]

Nakano MM, Geng H, Nakano S, Kobayashi K. The nitric oxide-responsive regulator NsrR controls ResDE-dependent gene expression. J Bacteriol. 2006; 188:5878–5887. [PubMed: 16885456]

Nakano MM, Hoffmann T, Zhu Y, Jahn D. Nitrogen and oxygen regulation of *Bacillus subtilis nasDEF* encoding NADH-dependent nitrite reductase by TnrA and ResDE. J Bacteriol. 1998; 180:5344–5350. [PubMed: 9765565]

Nakano MM, Marahiel MA, Zuber P. Identification of a genetic locus required for biosynthesis of the lipopeptide antibiotic surfactin in *Bacillus subtilis*. J Bacteriol. 1988; 170:5662–5668. [PubMed: 2848009]

Nakano MM, Zhu Y, LaCelle M, Zhang X, Hulett FM. Interaction of ResD with regulatory regions of anaerobically induced genes in *Bacillus subtilis*. Mol Microbiol. 2000; 37:1198–1207. [PubMed: 10972836]

Nakano MM, Zuber P, Glaser P, Danchin A, Hulett FM. Two-component regulatory proteins ResD-ResE are required for transcriptional activation of *fnr* upon oxygen limitation in *Bacillus subtilis*. J Bacteriol. 1996; 178:3796–3802. [PubMed: 8682783]

Nesbit AD, Giel JL, Rose JC, Kiley PJ. Sequence-specific binding to a subset of IscR-regulated promoters does not require IscR Fe-S cluster ligation. J Mol Biol. 2009; 387:28–41. [PubMed: 19361432]

Newton GL, Rawat M, La Clair JJ, Jothivasan VK, Budiarto T, Hamilton CJ, Claiborne A, Helmann JD, Fahey RC. Bacillithiol is an antioxidant thiol produced in Bacilli. Nat Chem Biol. 2009; 5:625–627. [PubMed: 19578333]

Overton TW, Whitehead R, Li Y, Snyder LA, Saunders NJ, Smith H, Cole JA. Coordinated regulation of the *Neisseria gonorrhoeae* truncated denitrification pathway by the nitric oxide-sensitive repressor, NsrR, and nitrite-insensitive NarQ-NarP. J Biol Chem. 2006; 281:33115–33126. [PubMed: 16954205]

Rankin LD, Bodenmiller DM, Partridge JD, Nishino SF, Spain JC, Spiro S. *Escherichia coli* NsrR regulates a pathway for the oxidation of 3-nitrotyramine to 4-hydroxy-3-nitrophenylacetate. J Bacteriol. 2008; 190:6170–6177. [PubMed: 18658270]

Reents H, Gruner I, Harmening U, Bottger LH, Layer G, Heathcote P, Trautwein AX, Jahn D, Hartig E. *Bacillus subtilis* Fnr senses oxygen via a [4Fe-4S] cluster coordinated by three cysteine residues without change in the oligomeric state. Mol Microbiol. 2006; 60:1432–1445. [PubMed: 16796679]

Rock JD, Thomson MJ, Read RC, Moir JW. Regulation of Denitrification Genes in *Neisseria meningitidis* by Nitric Oxide and the Repressor NsrR. J Bacteriol. 2007; 189:1138–1144. [PubMed: 17122348]

Rodionov DA I, Dubchak L, Arkin AP, Alm EJ, Gelfand MS. Dissimilatory metabolism of nitrogen oxides in bacteria: comparative reconstruction of transcriptional networks. PLoS Comput Biol. 2005; 1:e55. [PubMed: 16261196]

Schwartz CJ, Giel JL, Patschkowski T, Luther C, Ruzicka FJ, Beinert H, Kiley PJ. IscR, an Fe-S cluster-containing transcription factor, represses expression of *Escherichia coli* genes encoding Fe-S cluster assembly proteins. Proc Natl Acad Sci USA. 2001; 98:14895–14900. [PubMed: 11742080]

Song JY, Cha J, Lee J, Roe JH. Glutathione reductase and a mitochondrial thioredoxin play overlapping roles in maintaining iron-sulfur enzymes in fission yeast. Eukaryot Cell. 2006; 5:1857–1865. [PubMed: 16950927]

Spiro S. Regulators of bacterial responses to nitric oxide. FEMS Microbiol Rev. 2007; 31:193–211. [PubMed: 17313521]

Steinmetz M, Richter R. Plasmids designated to alter the antibiotic resistance expressed by insertion mutations *in Bacillus subtilis*, through in vivo recombination. Gene. 1994; 142:79–83. [PubMed: 8181761]

Sun G, Sharkova E, Chesnut R, Birkey S, Duggan MF, Sorokin A, Pujic P, Ehrlich SD, Hulett FM. Regulators of aerobic and anaerobic respiration in *Bacillus subtilis*. J Bacteriol. 1996; 178:1374–1385. [PubMed: 8631715]

Tucker NP, Hicks MG, Clarke TA, Crack JC, Chandra G, Le Brun NE, Dixon R, Hutchings MI. The transcriptional repressor protein NsrR senses nitric oxide directly via a [2Fe-2S] cluster. PLoS ONE. 2008; 3:e3623. [PubMed: 18989365]

Tucker NP, Le Brun NE, Dixon R, Hutchings MI. There's NO stopping NsrR, a global regulator of the bacterial NO stress response. Trends Microbiol. 2010; 18:149–156. [PubMed: 20167493]

Voskuil MI, Chambliss GH. The −16 region of *Bacillus subtilis* and other gram-positive bacterial promoters. Nucleic Acids Res. 1998; 26:3584–3590. [PubMed: 9671823]

Wang W, Richardson AR, Martens-Habbena W, Stahl DA, Fang FC, Hansen EJ. Identification of a repressor of a truncated denitrification pathway in *Moraxella catarrhalis*. J Bacteriol. 2008; 190:7762–7772. [PubMed: 18820017]

Weiss B. Evidence for mutagenesis by nitric oxide during nitrate metabolism in *Escherichia coli*. J Bacteriol. 2006; 188:829–833. [PubMed: 16428385]

Ye RW, Tao W, Bedzyk L, Young T, Chen M, Li L. Global gene expression profiles of *Bacillus subtilis* grown under anaerobic conditions. J Bacteriol. 2000; 182:4458–4465. [PubMed: 10913079]

Yeo WS, Lee JH, Lee KC, Roe JH. IscR acts as an activator in response to oxidative stress for the *suf* operon encoding Fe-S assembly proteins. Mol Microbiol. 2006; 61:206–218. [PubMed: 16824106]

Yukl ET, Elbaz MA, Nakano MM, Moënne-Loccoz P. Transcription factor NsrR from *Bacillus subtilis* senses nitric oxide with a 4Fe-4S cluster. Biochemistry. 2008; 47:13084–13092. [PubMed: 19006327]

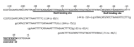

Figure 1.

Nucleotide sequence of the *nasD* regulatory region. The italicized adenine residues indicate the previously identified transcription start sites (Nakano *et al*., 1998). The sequence of the coding strand from −114 to +2 (relative to one of the transcription start sites) is shown. Underlined are the extended −10 element, the previously identified ResD-binding (Geng *et al*., 2004, Nakano *et al*., 2000) and NsrR-binding (Nakano *et al*., 2006) sites. The sequence of oligonucleotides used to generate EMSA probes are also listed. The numbers in the parentheses are relative to the transcription start site. The oligonucleotide marked with ++ indicates the site where [4Fe-4S]-NsrR preferentially binds with high affinity. Apo-NsrR binds to the regions marked with +, weakly binds to the site marked with ±, does not bind to the site marked with −.

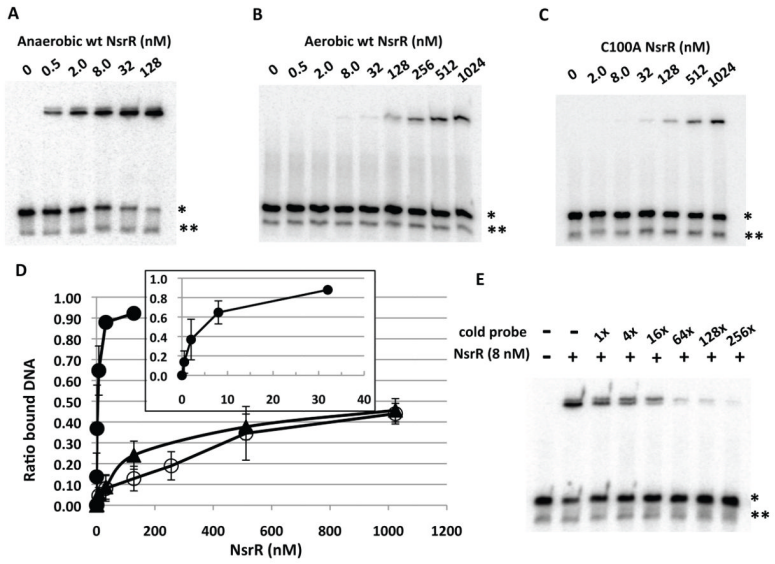

Figure 2.

Binding assay of NsrR to the *nasD* promoter. The sequence of the *nasD* probe (−44 to −19) that contains the proposed NsrR-binding site is shown in Figure 1. The radiolabelled probe (0.1 nM) was incubated with increasing concentrations of wild-type NsrR-His_6 purified under anaerobic conditions (A), aerobic conditions (B), or with the NsrR (C100A) mutant purified under anaerobic conditions (C). When anaerobically purified NsrR was used, the binding reaction as well as gel electrophoresis was carried out under anaerobic conditions as described in Experimental procedures. A single asterisk shows the double-stranded DNA and a double asterisk shows the single-stranded DNA, unannealed radiolabelled DNA oligonucleotide.

D. ImageJ was used to quantify the ratio of shifted band to total double-stranded probe bands from multiple EMSA experiments (n=6 for A and n=3 for B and C) and the average values are shown with standard deviations. Symbols: closed circles, anaerobically purified NsrR; open circles, aerobically purified NsrR; closed triangles, anaerobically purified NsrR(C100A) mutant protein. The inset shows a binding curve with anaerobic NsrR at concentrations less than 32 nM.

E. Competition assay. Anaerobically purified wild-type NsrR and radiolabelled *nasD* probe DNA were used with or without excess cold *nasD* DNA of the corresponding sequence.

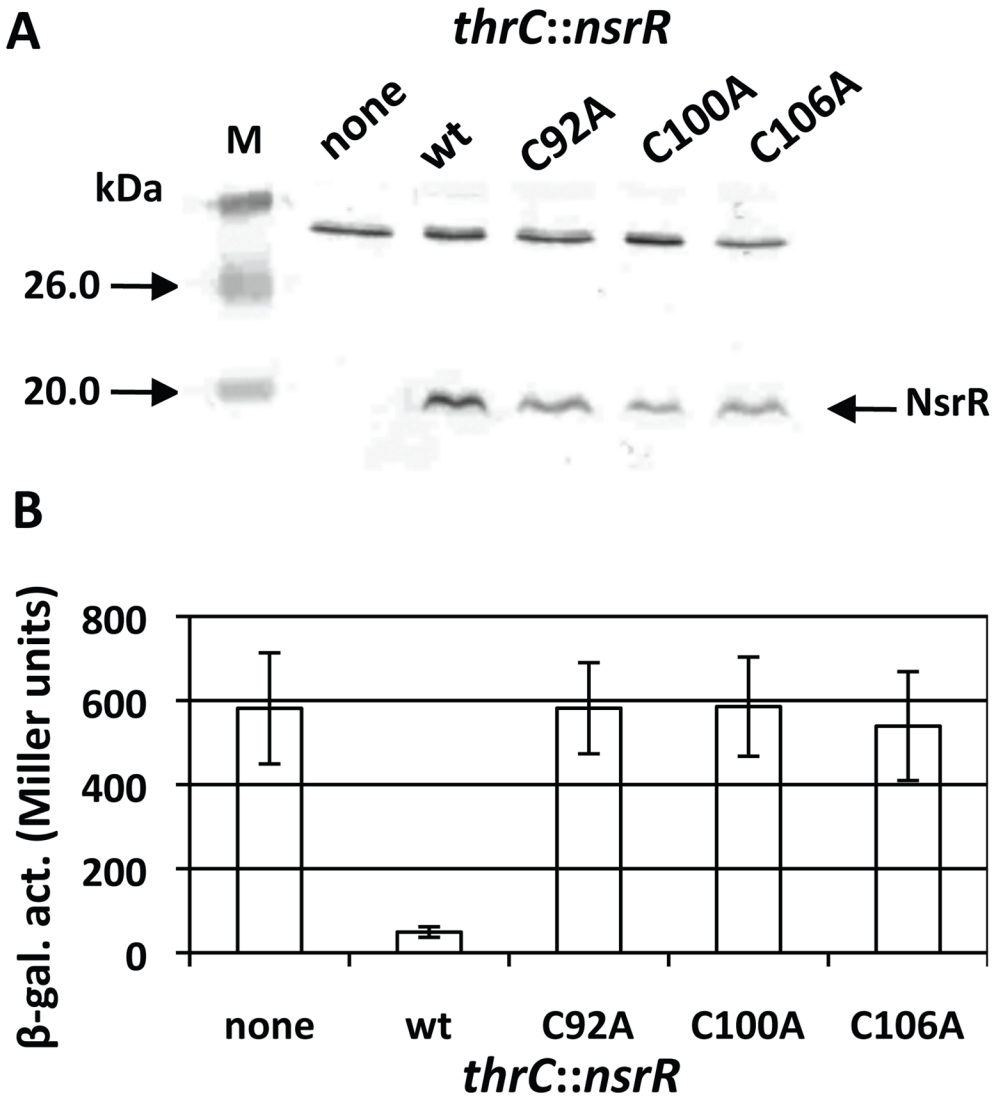

Figure 3.

Effect of cysteine mutations on *in vivo* NsrR activity.

A. Western blot analysis of the wild-type and mutant NsrR in *B. subtilis*. Cell lysate was prepared from a culture of an *nsrR* null mutant (none) as well as from the mutant carrying ectopically expressed wild-type *nsrR* (wt) or mutant alleles of *nsrR* (C92A, C100A, or C106A) at the *thrC* locus. The same amount of total protein from each lysate was resolved on an SDS-polyacrylamide gel and NsrR was detected by anti-NsrR antibody as described in Experimental procedures.

B. Strains carrying *nasD-lacZ* were grown in 2xYT supplemented with 0.5% glucose, 0.5% pyruvate, and appropriate antibiotics. Samples were collected at 1-h intervals to measure β-galactosidase activity and the activity at T1 (1 h after the end of exponential growth) is shown. The activities were measured at least three times in cultures of two independent clones and the average values of the data are presented along with standard deviations.

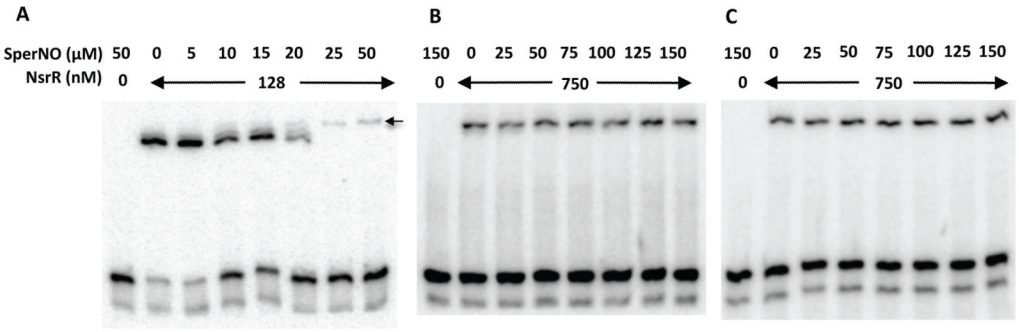

Figure 4.

Effect of spermine NONOate on DNA-binding activity of NsrR. The *nasD* DNA (−44 to −19) was incubated with indicated concentrations of either wild-type NsrR-His_6 purified under anaerobic conditions (A), aerobic conditions (B), or C100A mutant NsrR (C). Increasing concentrations of SperNO were added to the reaction as indicated. EMSA reactions and electrophoresis were carried out in an anaerobic chamber as described in Experimental procedures.

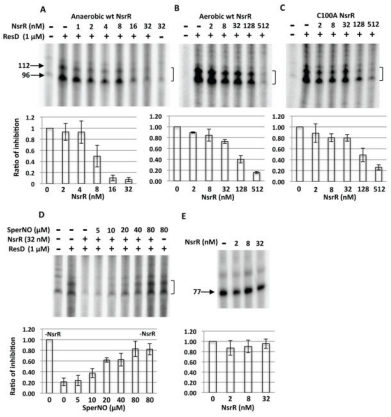

Figure 5.

In vitro transcription of *nasD*. The *nasD* template (−170 to +96) was incubated without or with σ^ARNAP, ResD~P (1 μM) and increasing concentrations of wild-type NsrR-His_6 purified under anaerobic conditions (A), aerobic conditions (B) or C100A mutant NsrR (C). An arrow with numbers shows the size of transcript in nucleotides. A bracket shows two *nasD* transcripts (96 and 112 base) that are generated by transcription *in vitro* as previously described (Geng *et al*., 2004) and the 96-base transcript corresponding to RNA transcribed *in vivo*.

D. Effect of spermine NONOate on repressor activity of NsrR. SperNO at the indicated concentration was added in the reaction with anaerobically purified NsrR.

E. *In vitro* transcription of *rpsD* using anaerobically purified NsrR. The 77 base transcript is marked.

The intensity of the corresponding bands was quantified with ImageJ and is shown as the ratio of transcript level in the presence of NsrR to that in the absence of NsrR (A, B, C and E), or as the ratio of transcript level in the presence of NsrR (and SperNO) to that in the absence of NsrR/SperNO (D). The average values (n=6 for A and n=3 for the rest) are shown with standard deviation.

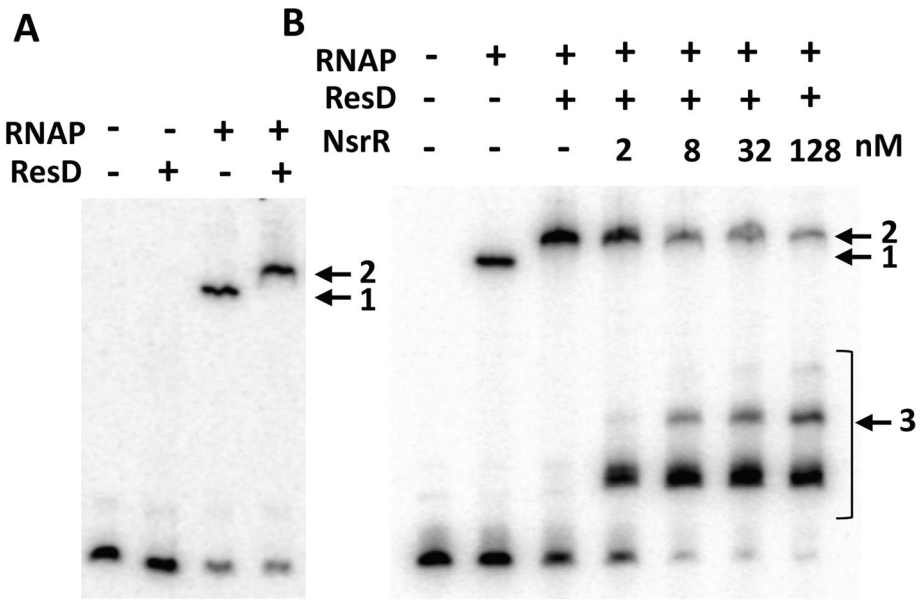

Figure 6.

Analysis of RNAP, ResD~P, and NsrR binding to the *nasD* promoter. The *nasD* probe encompassing −114 and −4 of the promoter region was used. All EMSA reactions and electrophoresis were carried out in an anaerobic chamber.

A. The probe (0.2 nM) was incubated with 0.5 μM ResD phosphorylated with 0.5 μM ResE, 15 nM RNAP, or both.

B. The probe was incubated with 15 nM RNAP in the absence or presence of 0.5 μM ResD~P and increasing concentrations of NsrR-His_6 purified under anaerobic conditions.

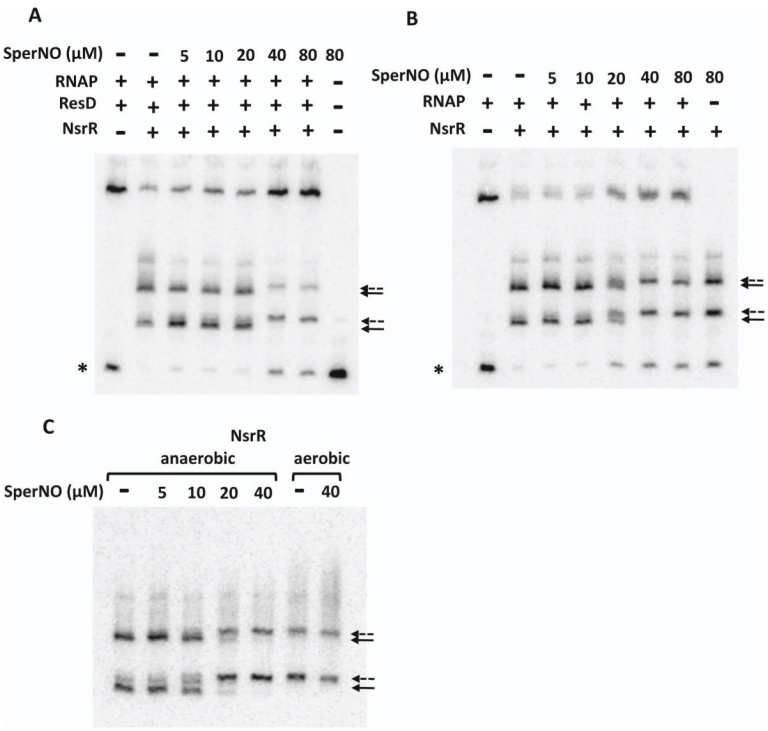

Figure 7.

Effect of spermine NONOate on DNA-binding activity of NsrR. The *nasD* (−114 to −4) probe was incubated with RNAP (15 nM), ResD~P (0.5 μM), and anaerobically purified NsrR-His_6 (128 nM) (A), or with RNAP and NsrR-His_6 (B) in the absence or presence of increasing concentrations of SperNO. Full arrows and broken arrows show the *nasD*-NsrR complex formed in the absence and presence of SperNO, respectively. A single asterisk shows the free probe.

C. The *nasD* probe was incubated with either anaerobically or aerobically purified NsrR-His_6 in the absence or presence of SperNO. The free probe ran off the gel. All EMSA reactions and electrophoresis were carried out in an anaerobic chamber.

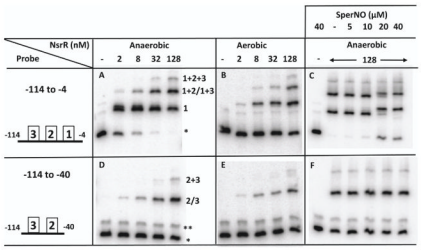

Figure 8.

Binding of NsrR to the *nasD* promoter with or without the primary NsrR-binding site. Two *nasD* DNA fragments were used for probes, one of which (−114 to −4) contains the primary NsrR-binding site, and the other (−114 to −40) lacks the binding site. Increasing concentrations of anaerobically or aerobically purified NsrR-His_6 and SperNO were used as indicated. A single asterisk shows a free probe and a double asterisk shows an unidentified DNA fragment generated in small amounts by PCR (note that this DNA does not bind to NsrR). Schematic views of the probe are shown in the leftmost panels and include the primary NsrR-binding site (marked with boxed 1) and secondary binding sites (marked with boxed 2 and 3). The three shifted bands in panel A correspond to the NsrR complexes interacting with the binding site 1 (shown as 1), binding site 1 and 2 or 1 and 3 (1+2/1+3), and the binding site 1, 2, and 3 (1+2+3) of the *nasD* probe. The two shifted bands in panel D correspond to the NsrR complexes interacting with the binding site 2 or 3 (2/3), and the binding site 2 and 3 (2+3).

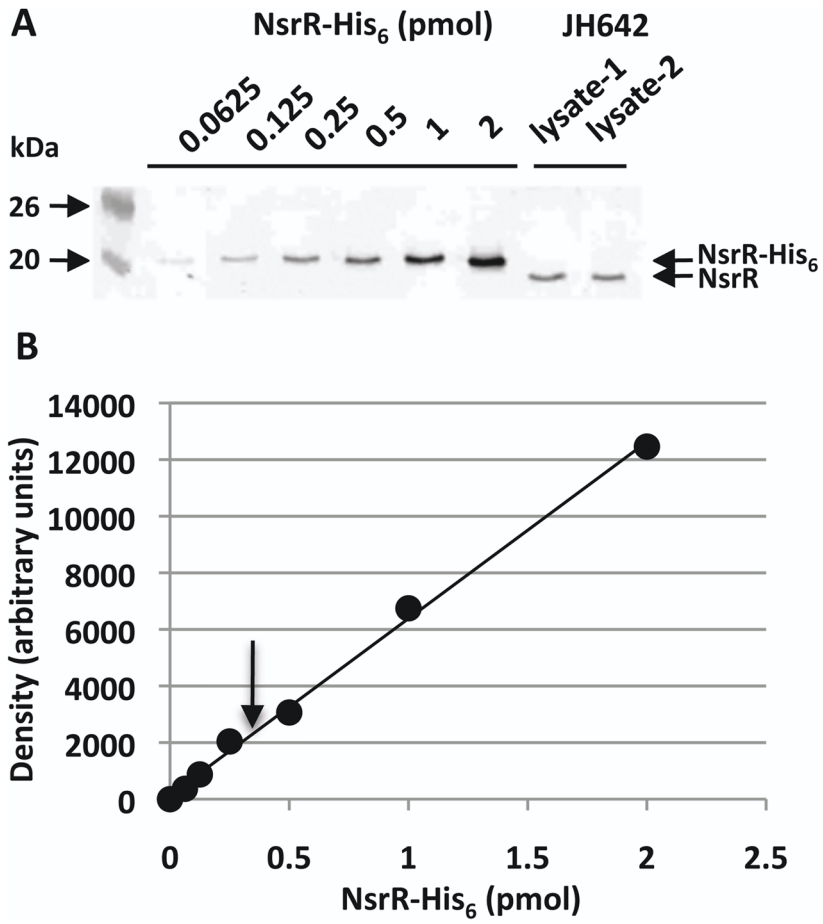

Figure 9.

Determination of *in vivo* NsrR concentration in *B. subtilis* cells using quantitative western blot analysis.

A. Western blot of increasing amounts of purified NsrR-His_6 together with *B. subtilis* cell lysate pepared from independent cultures. Molecular weight markers are marked.

B. The standard curve was plotted by quantifying band densitities of NsrR-His_6 shown in panel A. An arrow indicates the intensity of NsrR detected in the cell lysate shown in panel A.